Using CFD Software to Calculate Hydrodynamic Coefficients

He Zhang[*], Yu-ru Xu and Hao-peng Cai

Key Laboratory of Science and Technology for National Defense of Autonomous Underwater Vehicle,
Harbin Engineering University, Harbin 150001, China

Abstract: Applications of computational fluid dynamic (CFD) to the maritime industry continue to grow with the increasing development of computers. Numerical approaches have evolved to a level of accuracy which allows them to be applied for hydrodynamic computations in industry areas. Hydrodynamic tests, especially planar-motion-mechanism (PMM) tests are simulated by CFD software –FLUENT, and all of the corresponding hydrodynamic coefficients are obtained, which satisfy the need of establishing the simulation system to evaluate maneuverability of vehicles during the autonomous underwater vehicle scheme design stage. The established simulation system performed well in tests.

Keywords: FLUENT; planar-motion-mechanism (PMM); hydrodynamic coefficients; motion simulation

Article ID: 1671-9433(2010)02-0149-07

1 Introduction

Autonomous underwater vehicle (AUV) is a kind of submarine vehicle that works in deep water which is of a range from tens to thousands of meters depth where its maneuverability almost has no influence on free water surface, wave-making(Xu *et al*., 2006). In recent years, there have been intensive efforts toward the development of AUV (Wernli, 2002). To design an AUV, its maneuverability and controllability must be examined in advance preferably based on a mathematical model. The mathematical model contains hydrodynamic forces and moments expressed in terms of hydrodynamic coefficients. Therefore, it is important to know the values of these coefficients to simulate the performance of the AUV accurately.

The hydrodynamic coefficients may be classified into three types: linear damping coefficients, linear inertial force coefficients, and nonlinear damping coefficients. Among these coefficients, the linear damping ones affect AUV's maneuverability mostly when AUV navigates in steady-state flow (Sen, 2000); while in unsteady-state flow, linear inertial force coefficients and nonlinear ones must be taken into consideration too. These coefficients are usually determined by experiments, numerical analysis, system identification or empirical formula. Because of numbers of appendage and variant shape of AUVs' bodies, there is no systematic design information which could be used to estimate coefficients of AUV yet. When estimation work of AUV is completed according to the empirical formula for ship, submarine and torpedo, a mass of errors are unavoidable. The method of system identification performs well in navigation data

analyses and hydrodynamic coefficients correction, but it doesn't work well during the AUV maneuverability design stage (Hu Z Q, 2007). Although planar-motion-mechanism (PMM) tests are the most popular ones among all of the experimental hydrodynamic tests, measured data from these tests are not completely reliable because of experimental difficulties and errors involved, meanwhile tests cost lots of time and money.

With the increasing development of computers, applications of CFD in the maritime industry are feasible and important. Numerical approaches have evolved to a level of accuracy which allows them to be applied to practical ship resistance and propulsion computations in industry areas. In recent years, CFD is also being applied to determine some of hydrodynamic coefficients that are needed in evaluating maneuvering characteristics of marine vehicles (Ferziger and Peric, 2002; Sarkar *et al*., 1997; Wilson *et al*., 2006; Tyagi A *et al*., 2006).

In this paper, a new method using CFD software FLUENT to simulate hydrodynamic tests is presented and then hydrodynamic coefficients which are needed in establishing hydrodynamic model are calculated. The new calculation method is convenient, low-cost, and clean. The well-performed maneuverability prediction results obtained by this motion simulation system have proven that the calculated hydrodynamic coefficients could satisfy the design requirement of maneuverability and prediction during the AUV scheme design stage.

This paper is organized as follows: Section II describes the LEUV model and basic calculation theory. Section III presents the new method of simulating hydrodynamic tests using FLUENT and calculation results. Section IV establishes AUV's motion simulation system. Section V shows maneuverability prediction results. Finally, Section

VI presents conclusions.

2 Basic theory

2.1 Description of the model

The object studied in this paper is a long-endurance underwater vehicle (LEUV) which can work in a wide-range sea area and deal with complex tasks.

The entity model is a spheroid-shaped vehicle with four horizontal wings and a vertical rudder. According to the entity model, calculation model was established using GAMBIT with a scale of 1:1 (Fig.1), and then corresponding domain and designing gird were established.
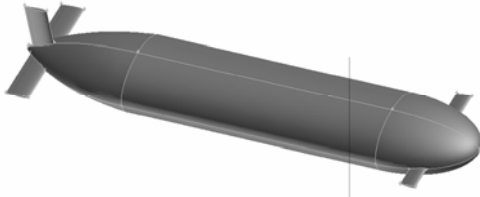

Fig.1 Entity model of LEUV

The proportion between cuboids solution domain and the model is set to 7:1 in order to simulate the vehicle navigation in deep sea area (Fig.2). The number of the calculation model girds which are triangular unstructured ones is 413 565. The number has been conformed after several trials and calculations. The distribution of girds is shown in Fig.2.
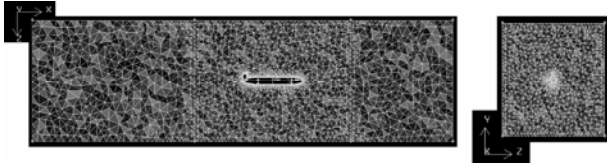

Fig.2 Girds distribution of LEUV

2.2 Governing equation

A model was established in order to solve the problem caused by flow around the vehicle. The model is based on the Reynolds Averaged Navier–Stokes (RANS) equations. For a turbulent flow, the velocity field and pressure field can be decomposed into two parts: the mean (ensemble average) velocity and pressure $\langle u_i \rangle$ and $\langle p \rangle$, and the deviatoric (or turbulent) velocity and pressure u_i' and p'. Thus, $u_i = \langle u_i \rangle + u_i'$ and $p = \langle p \rangle + p'$, in which $i = 1, 2, 3$ for a 3-D flow. If the fluid is assumed incompressible, the mean flow field is governed by the RANS equations:

$$\frac{\partial U_j}{\partial x_j} = 0 \tag{1}$$

$$\frac{\partial U_i}{\partial t} + \frac{\partial}{\partial x_j}(U_i U_j) = -\frac{1}{\rho}\frac{\partial P}{\partial x_i} + \frac{1}{\rho}\frac{\partial}{\partial x_j}(\Gamma_{ij} - \rho \overline{u_i' u_j'}) \tag{2}$$

In which ρ is the density of the fluid, Reynolds stress tensor is

$$-\rho \overline{u_i' u_j'} = \begin{bmatrix} -\rho \overline{u_1'^2} & -\rho \overline{u_1' u_2'} & -\rho \overline{u_1' u_3'} \\ -\rho \overline{u_2' u_1'} & -\rho \overline{u_2'^2} & -\rho \overline{u_2' u_3'} \\ -\rho \overline{u_3' u_1'} & -\rho \overline{u_3' u_2'} & -\rho \overline{u_3'^2} \end{bmatrix}$$

2.3 Turbulent model

The $k-\varepsilon$ SST, $k-\varepsilon$ hereafter, and Reynolds stress transport, RSTM hereafter, turbulence models are used for turbulence closure in the present study. The $k-\varepsilon$ model is one of the most widely used turbulence models for external aerodynamics and hydrodynamics. $k-\varepsilon$ model is chosen as turbulent model in this paper.

k function:

$$\frac{\partial \rho k}{\partial t} + \nabla \bullet (\rho \bar{U} k) = \nabla \bullet [(\mu + \frac{\mu_t}{\sigma_k})\nabla k] + P_k - \rho \varepsilon \tag{3}$$

ε function:

$$\frac{\partial \rho \varepsilon}{\partial t} + \nabla \bullet (\rho \bar{U} \varepsilon) = \nabla \bullet [(\mu + \frac{\mu_t}{\sigma_k})\nabla \varepsilon] + \frac{\varepsilon}{k}(C_{\varepsilon 1} P_k - C_{\varepsilon 2} \rho \varepsilon) \tag{4}$$

where,

$$P_k = \mu_t \nabla \bar{U} \bullet (\nabla \bar{U} + \nabla \bar{U}^T) - \frac{2}{3}\nabla \bullet \bar{U}[(3\mu_t \nabla \bullet \bar{U} + \rho k)]$$

$$\mu_t = C_\mu \rho \frac{k^2}{\varepsilon}$$

2.4 Boundary conditions

Set boundary conditions in preprocess software GAMBIT:
(1) inflow (right boundary of solution domain): velocity inlet;
(2) outflow (left boundary of solution domain): outflow;
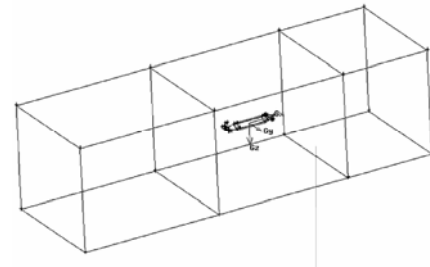(3) wall (surface of the vehicle): wall;
(4) fluid domain: FLUID.

Fig.3 Space distribution of vehicle and domain

3 Simulation hydrodynamic tests using FLUENT

Simulation tests proposed in this paper conclude two kinds of conditions: steady-state and unsteady-state. Unsteady-state tests include five maneuverability tests that operated with PMM, while the steady-state ones are linear motion and loxodromic motion tests.

3.1 Simulating unsteady-state tests

3.1.1 Setting initialization

Simulation tests are completed using FLUENT software. Some parameters are set as follows. Choose the first order implicit solver, standard $k-\varepsilon$ model, standard wall function; the other options remain as default. SIMPLE algorithm is used to calculate pressure-velocity coupling. Pressure discretization is PRESTO!, Momentum discretization is the second order Upwind, and the other ones are the first order Upwind. Force and momentum data are recorded in every step.

3.1.2 Using dynamic meshes

There are two kinds of User Defined Function (UDF) for simulating PMM tests— translation ones and rotation ones according to the characteristic of tests. UDF is programmed to make the wall of the vehicle model moving as motion equation in the solution domain.

Take the heave motion test as an example (translation UDF),

$$\begin{cases} \xi = a\sin\omega t \\ \theta = \dot{\theta} = 0 \\ w = \dot{\xi} = a\omega\cos\omega t \\ \dot{w} = -a\omega^2\sin\omega t \end{cases} \quad (5)$$

where ξ -vertical displacement of AUV model;

a -amplitude of the heave motion of AUV model;

ω -circular frequency of heave motion of AUV model;

$\theta, \dot{\theta}$ -angle and angular velocity rotated along y axis;

$w, \dot{w}$ -vertical velocity and acceleration.

Take the pitch motion test as an example (rotation UDF),

$$\begin{cases} \theta = \theta_0\sin\omega t \\ q = \dot{\theta} = \theta_0\omega\cos\omega t \\ \dot{q} = -\theta_0\omega^2\sin\omega t \\ w = \dot{w} = 0 \end{cases} \quad (6)$$

where $\theta, \dot{\theta}$ -angle and angular velocity rotated along y axis;

$q, \dot{q}$ - angle and angular velocity in pitch motion;

ω -circular frequency of pitch motion of AUV model;

$w, \dot{w}$ -vertical velocity and acceleration.

The numerical tests follow the rules hereinafter. The vehicle surges in the solution domain at different frequencies (0.2 Hz, 0.25 Hz, 0.3125 Hz, 0.4 Hz, 0.5 Hz, 0.625 Hz, and 0.8 Hz) and its amplitude is 0.04 m. The parameters are nondimensionalized with inlet velocity 1 m/s and characteristic length L. One motion period is divided into 400 steps during the calculation.

3.1.3 Data processing

Simulation calculation goes on 6~7 cycles to get stable curves of force and moment with time in disregard of oscillation from the beginning. The mean value of the last three cycles stable data is used for post-processing. Replace the characteristic length by the supposed area value when doing the non-dimensional work.

Results derived from FLUENT software are a series of discrete points that are $f(t)$ with regard to t .

$$f(t) = \frac{a_0}{2} + a_1\cos\omega t + b_1\sin\omega t \quad (7)$$

namely, $$Z' = Z_a\sin\omega t + Z_b\cos\omega t + Z_0' \quad (8)$$

$$M' = M_a\sin\omega t + M_b\cos\omega t + M_0' \quad (9)$$

where, L is the characteristic length of model, V is the incoming flow velocity.

$$Z_a = -\frac{a\omega^2 L}{V^2}Z_{\dot{w}}'; \; Z_b = \frac{a\omega}{V^2}Z_w'; \quad (10)$$

$$M_a = -\frac{a\omega^2 L}{V^2}M_{\dot{w}}'; \; M_b = \frac{a\omega}{V^2}M_w' \quad (11)$$

According to the formulae above, deal with the result data as Fourier expansion using MATLAB software, then derive Z_a , Z_b , M_a , M_b , furthermore derive relevant hydrodynamic coefficients from each motion of PMM tests. Then, PMM simulation tests are completed.

3.2 Simulating steady-state tests

3.2.1 Setting initialization

Simulating steady-state tests are completed using FLUENT software and some parameters are set as follows. Choose the first order implicit solver with steady option (K and Epsilon, parameter Turbulent Kinetic Energy=1 m²/s³, Turbulent Dissipation Rate=1 m²/s³), standard wall function, while other options remain default, without energy function. SIMPLE algorithm is used to calculate pressure-velocity coupling, pressure discretization is the first order upwind discrete mode, and momentum discretization is the first order upwind discrete mode. Force and momentum data are recorded in every step.

3.2.2 Simulation of linear test

The vehicle buoys flat in the solution domain, magnitude of longitudinal forces are recorded with velocity series. On the basis of data above, the longitudinal resistance coefficient could be calculated. Operation condition in the flame restricts the simulating inlet flow velocity varying from 0.3 to 1.7 m/s with an increment of 0.1 m/s.

3.2.3 Simulation of loxodrome test

When simulating loxodrome test, set horizontal inlet flow at the inlet of the domain and then rotate the model in the

domain as the attack angle of the plane which varies from -10° to 10° with an increment of 2°. Hold the horizontal velocity at a constant, and record force and moment of the loxodrome test. Deal with the data so as to calculate the corresponding hydrodynamic coefficients.

3.3 Calculation results

All the simulating tests are completed in the first two sections of this chapter. Hydrodynamic coefficients are presented here in Table 1.

Based on the coefficients presented in Table 1, 24 other coefficients can be derived according to correlative article (Shi, 1995).

Table 1 Calculated hydrodynamic coefficients

Coefficient	FLUENT	Coefficient	FLUENT
$Z'_{\dot{w}}$	-0.04575	Z'_q	0.000494
Z'_w	-0.3376	$Z'_{\dot{q}}$	-0.01656
$M'_{\dot{w}}$	0.00053	$M'_{\dot{q}}$	-0.00253
M'_w	0.0366	M'_q	-0.0366
$Y'_{\dot{v}}$	-0.01763	$Y'_{\dot{r}}$	-0.00016
Y'_v	-0.1081	Y'_r	0.03322
$N'_{\dot{v}}$	-0.000167	$N'_{\dot{r}}$	-0.00073
N'_v	-0.00863	N'_r	-0.0093
$K'_{\dot{p}}$	-2.48E-05	Z'_w	-0.148
K'_p	-5.17E-04	$Z'_{w|w|}$	-0.06588
Y'_v	-0.0525	$Y'_{v|v|}$	-0.0091

4 Design of motion simulation system

4.1 Definition of the coordinate system

In order to describe the motion of a vehicle, two coordinate systems are defined as shown in Fig.4. The linear displacement is represented in the earth-fixed frame, and the equations of motion are described in the body-fixed frame. Hydrodynamic forces acting on a ship can be easily described in the body-fixed frame than in other reference frames. The origin of the body-fixed frame is the cross point of the longitudinal center line, the water line, and the mid-ship section, and the positive z axis is downwards.
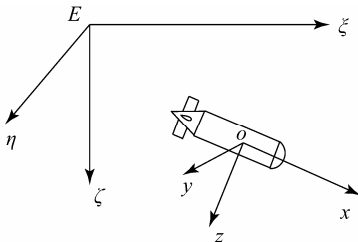

Fig.4 Definition of coordinate system and symbols

4.2 Six DOF mathematic model of AUV

The vehicle studied in this paper is LEUV with four propellers and four rudders and one wing. The first two propellers are the main propellers fixing at both sides of the astern body, while the other two are vertical propellers fixing at the fore and aft along the main axis. This kind of propulsive system causes less amplitude in roll motion.

In nonlinear observers, 6 DOF AUV equations of motion and the augmented states for the linear damping coefficients are included. Thus, the observer model describes surge, sway, heave, roll, pitch, and yaw motions. The coordinate system is shown in Fig.4. The 6 DOF equations of motion for the observer model are as follows:

$$\text{Surge}: \left[m \times (\dot{u}_r - v_r r + w_r q) - x_G \times (q^2 + r^2) + y_G(pq - \dot{r}) + z_G(pr + \dot{q}) \right] = X_c$$

$$\text{Sway}: m \times \left[(\dot{v}_r - w_r p + u_r r) - y_G(r^2 + p^2) + z_G(qr - \dot{p}) + x_G(qp + \dot{r}) \right] = Y_c$$

$$\text{Heave}: m \times \left[(\dot{w}_r - u_r q + v_r p) - z_G(p^2 + q^2) + x_G(rp - \dot{q}) + y_G(rq + \dot{p}) \right] = Z_c$$

$$\text{Roll}: I_x \dot{p} + (I_z - I_y)qr + m \left[y_G(\dot{w}_r + pv_r - qu_r) - z_G(\dot{v}_r + ru_r - pw_r) \right] = K_c$$

$$\text{Pitch}: I_y \dot{q} + (I_x - I_z)rp + m \times \left[z_G \times (\dot{u}_r + w_r q - v_r r) - x_G \times (\dot{w}_r + pv_r - u_r q) \right] = M_c$$

$$\text{Yaw}: I_z \dot{r} + (I_y - I_z)pq + m \times \left[x_G \times (\dot{v}_r + u_r r - p_r w) - y_G \times (\dot{u}_r + qw_r - v_r r) \right] = N_c$$

(12)

where u, v, and w are the velocity of surge, sway, and heave motion, p, q, and r are angular velocity of roll, pitch, and yaw motion, respectively. X, Y, Z, K, M, and N represent the resultant forces and moments with respect to x, y, and z axis.

Exterior forces of AUV in current are in the left side of the motion function, described as $F_C = [X_c, Y_c, Z_c, K_c, M_c, N_c]^T$. There are some kinds of forces acting on the AUV through force analysis: hydrodynamic force, thrust force, gravity, buoyancy etc. Gravity equals to buoyancy, while trust force is considered as other exterior force. Simulating each force as follows:

Hydrodynamic force: The force is available from hydrodynamic tests of model, and then transforms it to the entity model.

Propulsive forces: Thruster force T is related with propeller rate of rotation according to propeller theory.

$$T = f(n) \qquad (13)$$

The propeller rate of rotation is gotten from the last minute's thruster simulation value. Obtaining the propeller thrust by interpolating the curve of $T - n$.

Rudder forces: Because of the eudipleural shape of rudders, hydrodynamic force caused by rudder is a function of rudder angle δ, where $X(\delta)$ is even function, $Y(\delta)$ and $N(\delta)$ are odd function. Besides, performance of rudder is greatly influenced by yaw angular velocity r, the existence of r changes the rudder's effective hydrodynamic angle. Therefore, the calculation of rudder forces and moments are as follows:

$$Y(\delta, r) = Y_\delta \delta + Y_r r + Y_{|r|\delta} |r| \delta \qquad (14)$$

$$N(\delta, r) = N_\delta \delta + N_r r + N_{|r|\delta} |r| \delta \qquad (15)$$

Wave forces: The calculation of relative velocity of wave is put firstly.

$$
\begin{aligned}
u_r &= u - U_c \cos\theta \cos(\alpha_c - \psi) \\
v_r &= v - U_c \sin(\alpha_c - \psi) \\
w_r &= w - U_c \sin\theta \cos(\alpha_c - \psi)
\end{aligned}
\qquad (16)
$$

And then the functions above are put in the motion equation after being differentiated to simulate the wave effect.

Consequently, the inertial hydrodynamic force is transferred to the left side of motion equation, while non-inertial one is in the other side of the equation, and then the observer model (12) is transformed into state matrix form. When $t \in [t_i, t_{i+1})$, $i = 0,1,2\cdots,\infty$,

$$E\dot{X} = F_{visCi} + F_{TCi} \qquad (17)$$

Similarly,

$$\dot{X}_R = E^{-1}(F_{visCi} + F_{TCi}) \qquad (18)$$

where $X_R = [u,v,w,p,q,r]^T$ is relative velocity in the body coordinate, F_{vicCi} is non-inertial hydrodynamic force, E is the matrix coefficient. F_{vicCi}, F_{TCi} are the function of U_{rm} respectively when the motion is in wave.

$$
E = \begin{bmatrix}
m - X_u & 0 & 0 & 0 & mz_G & 0 \\
0 & m - Y_v & 0 & -mz_G - Y_p & 0 & mx_G - Y_r \\
0 & 0 & m - Z_w & 0 & -mx_G - Z_q & 0 \\
0 & -mz_G - K_v & 0 & I_x - K_p & 0 & -K_r \\
mz_G & 0 & -mx_G - M_w & 0 & I_y - M_q & 0 \\
0 & mx_G - N_v & 0 & -N_p & 0 & I_z - N_r
\end{bmatrix}
$$

Therefore, nonlinear observers are designed based on Eq.(17).

4.3 Establishing simulation system
According to the motion equations, 6 DOF AUV simulation system enclosing several modules includes force module, inertial coefficient module, acceleration module and current state module, as shown in Fig.5. This kind of package technology can improve the program portability and reusage of this simulation system.
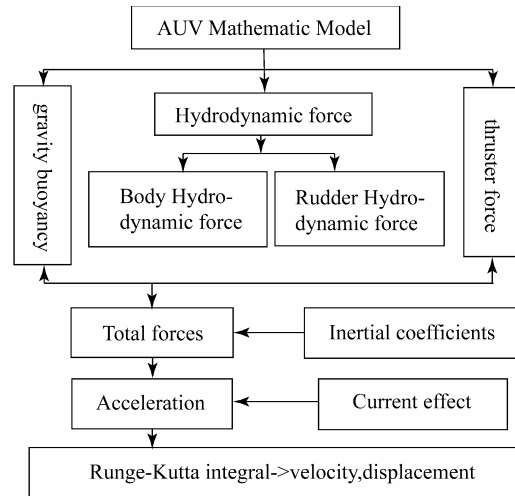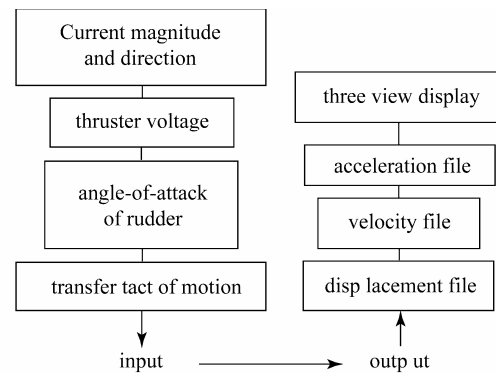

Fig.5 The flow chart of motion simulation system

Fig.6 The operating flow chart of motion simulation system

5 Hydrodynamic prediction results by simulation system

Using the mathematics model of LEUV as described in Chapter 4, standard maneuvering tests such as turning circle tests and Zigzag tests are carried out.

5.1 Straight course in horizontal plane
Taking no account of the influence of wave, the voltage of two main propellers varies from 1V to 5V with an increment of 1V.
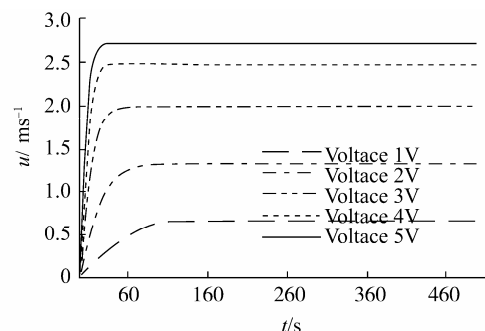

Fig.7 The chart of velocity

In Fig.7, the longitudinal velocity changes in time following each voltage. As shown in the figure, the time cost to maintain a stable velocity is shorter with the increase of the voltage loaded on the propellers.

5.2 Turning motion on horizontal plane

The voltage of the main propeller is set at 5V, in disregard of wave influence. The curve of centrobaric trajectory on horizontal plane is shown in Fig.8. As shown in the figure bellow, the maneuverable time of the vehicle is decreasing and the turning radius is shortening with the increment of rudder deflection.
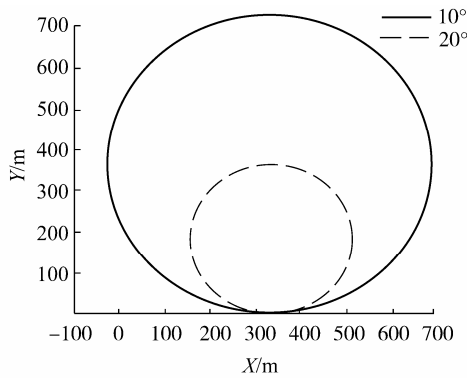

Fig.8 The curve of centrobaric trajectory

5.3 Zigzag motion on horizontal plane

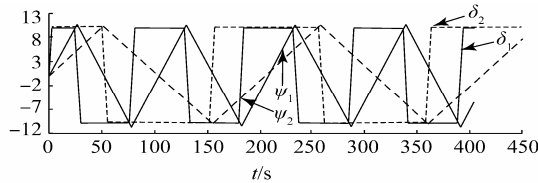$10° - 10°$ and $5° - 5°$ Zigzag tests are shown in Figs. 9~12.

Fig.9 The curve of Ψ, δ in $10° - 10°$ Zigzag motion
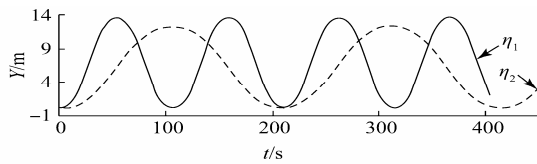
Fig.10 The curve of centrobaric trajectory in $10° - 10°$ Zigzag motion
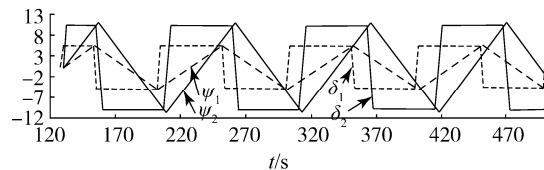

Fig.11 The curve of Ψ, δ in $5° - 5° / 10° - 10°$ Zigzag motion
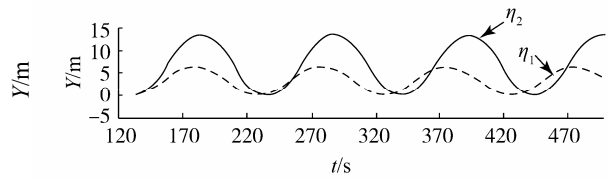

Fig.12 The curve of centrobaric trajectory in $5° - 5° / 10° - 10°$ Zigzag motion

The influence of the shape of LEUV on its maneuverability could be reflected in these figures above. The increase of δ has little influence on the period of Zigzag, but the change value of over angle θ_{ov} has increased.

The results of standard maneuvering tests above show that the simulation system established is available and can be used as a tool to predict the maneuverability of AUV.

6 Conclusions

The first part of this paper presents a new method using CFD software FLUENT to simulate hydrodynamic tests, especially PMM tests and their post-progress. All of the corresponding hydrodynamic coefficients are obtained. In the second part of this paper, a simulation system has been established, consisting of force module, inertial coefficient module, acceleration module and current state module. This system could satisfy the need to predict the maneuverability of AUV during scheme design stage together with the usage of coefficients obtained above. Results of several simulated standard maneuvering tests have proven that the precise level of these coefficients can satisfy the need of establishing AUV's simulation system and the simulation system also provides a platform for the automatic control and debug.

The method of doing hydrodynamic tests by computer presented in this paper provides a new method and means to calculate hydrodynamic coefficients. The method has the advantages over traditional flume hydrodynamic tests; moreover, it is low-cost, clean, effective and independent of the condition of experimental equipment and the human-caused error.

References

Ferziger JH, Peric M (2002). *Computational method for fluid dynamics*, Springer, Berlin, 28-50.

Hu ZQ, Lin Y, Gu HT (2007). On numerical computation of viscous hydrodynamics of unmanned underwater vehicle. *Robot*, **2**(5), 145-150.

Sarkar T, Sayer P G, Fraser S M (1997). A study of autonomous underwater vehicle hull forms using computational fluid dynamics. *International Journal for Numerical Methods in Fluids*, **25**(11), 1301-1313.

Sen D (2000). A study on sensitivity of maneuverability performance on the hydrodynamic coefficients for submerged

bodies. *Journal of Ship Research*, **44**(3), 186–196.

Shi S D (1995). *Submarine Maneuverability*. National Defense Industry Press, Beijing, 50-78.

Tyagi A, Sen D (2006). Calculation of transverse hydrodynamic coefficients using computational fluid dynamic approach. *Ocean Engineering*, **33**(5), 798-809.

Wernli RL (2002). AUVs--A technology whose time has come. *Proc. Conf. UT'02 OES/IEEE*, 309–314.

Wilson R, Paterson E, Stern F (2006). Unsteady RANS CFD method for naval combatant in waves. *Proceedings of the 22nd ONR Symposium on Naval Hydrodynamics*, Washington DC, National Academy Press, 532-549.

Xu YR., Su YM, Pang Y J (2006). Expectation of the development in the technology on ocean space intelligent unmanned vehicles. *Chinese Journal of Ship Research*, 3(1), 1-4.

He Zhang was born 1982. She is currently working toward her Ph.D degree in the Design and Construction of Naval Architecture at Harbin Engineering University. Her current research interests include hydrodynamic calculation, image processing, *etc*.

Yu-ru Xu was born 1942. He is an academician of CAE and a professor of Harbin Engineering University. His current research interests include AUV technique, *etc*.
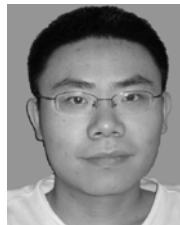
Hao-peng Cai was born 1983. He is currently working toward his Ph.D degree in the Design and Construction of Naval Architecture at Harbin Engineering University. His current research interests include hydrodynamic calculation, *etc*.